Branching tree model with fractal vascular resistance explains fractal perfusion heterogeneity

M. Marxen and R. M. Henkelman

AJP - Heart 284:1848-1857, 2003. First published Jan 16, 2003; doi:10.1152/ajpheart.00510.2002

AJP - Heart and Circulatory Physiology publishes original investigations on the physiology of the heart, blood vessels, and lymphatics, including experimental and theoretical studies of cardiovascular function at all levels of organization ranging from the intact animal to the cellular, subcellular, and molecular levels. It is published 12 times a year (monthly) by the American Physiological Society, 9650 Rockville Pike, Bethesda MD 20814-3991. Copyright © 2005 by the American Physiological Society. ISSN: 0363-6135, ESSN: 1522-1539. Visit our website at http://www.the-aps.org/.

Am J Physiol Heart Circ Physiol 284: H1848–H1857, 2003.
First published January 16, 2003; 10.1152/ajpheart.00510.2002.

Branching tree model with fractal vascular resistance explains fractal perfusion heterogeneity

M. Marxen and R. M. Henkelman
Department of Medical Biophysics, Sunnybrook and Women's College Health Sciences Centre, University of Toronto, Toronto, Ontario, Canada, M4N 3M5

Submitted 20 June 2002; accepted in final form 8 January 2003

Marxen, M., and R. M. Henkelman. Branching tree model with fractal vascular resistance explains fractal perfusion heterogeneity. *Am J Physiol Heart Circ Physiol* 284: H1848–H1857, 2003. First published January 16, 2003; 10.1152/ajpheart.00510.2002.—Perfusion heterogeneities in organs such as the heart obey a power law as a function of scale, a behavior termed "fractal." An explanation of why vascular systems produce such a specific perfusion pattern is still lacking. An intuitive branching tree model is presented that reveals how this behavior can be generated as a consequence of scale-independent branching asymmetry and fractal vessel resistance. Comparison of computer simulations to experimental data from the sheep heart shows that the values of the two free model parameters are realistic. Branching asymmetry within the model is defined by the relative tissue volume being fed by each branch. Vessel ordering for fractal analysis of morphology based on fed or drained tissue volumes is preferable to the commonly used Strahler system, which is shown to depend on branching asymmetry. Recently, noninvasive imaging techniques such as PET and MRI have been used to measure perfusion heterogeneity. The model allows a physiological interpretation of the measured fractal parameters, which could in turn be used to characterize vascular morphology and function.

morphology; blood flow modeling; vessel ordering; imaging; asymmetry

PERFUSION IS DEFINED as the amount of blood delivered to a unit mass of tissue per unit time. Average perfusion of an organ can be calculated by dividing the flow through the supplying artery by the mass of the organ. However, local perfusion values within the organ have been found to vary significantly and to show positive correlation in space (1, 2, 17). This means that it is likely that the area surrounding a highly perfused region of the organ is also highly perfused. More importantly, the correlation has been found to be independent of the size (scale) of the measurement volumes, which implies that perfusion heterogeneity is a self-similar or fractal quantity (2, 17). This statement is equivalent to the observation that perfusion heterogeneity as a function of scale can be described by a power law (see METHODS). Differences in local perfusion arise from differences in the resistance of the supplying vascular pathways. Consequently, we can learn something about vascular structure and resistance by measuring the heterogeneity and spatial correlation of perfusion.

Recently, imaging techniques such PET (8) and MRI (4) have been used to acquire data on perfusion heterogeneities. However, without a convincing model that establishes a link between the measured parameters and the underlying vascular structure, a physiologically useful interpretation of these measurements is difficult.

In this article, we present a model that suggests a connection between fractal perfusion heterogeneities and the scaling of vessel resistance as well as branching asymmetry. The model is based on the assumption of fractal vessel resistance, meaning that vessel resistance also obeys a power law as a function of scale similar to the heterogeneity of perfusion. The scale of an artery will be defined here as the volume of tissue that it supplies. This definition of scale also leads to a new approach to vessel ordering that is discussed in detail in METHODS. Branching asymmetry δ within the model is defined as the relative tissue volume fraction being fed by the smaller branch of a vessel bifurcation.

Vascular structure in the heart, as depicted in Fig. 1, features highly asymmetric vessel branching and large variations in the distances from the feeding artery to the terminal vessels. The model incorporates these features, and simulations demonstrate that the model is able to reproduce perfusion heterogeneity in the sheep heart as measured by Bassingthwaighte et al. (3) as well as morphological data from the human heart gathered by Zamir (20).

Certain computer-generated, three-dimensional vascular tree structures have been shown to reproduce perfusion heterogeneities similar to real physiological systems (5, 7, 11). However, the complexity of the generating algorithms may not be essential to account for the perfusion heterogeneity. No concrete morphological parameters have been identified as the cause of fractal perfusion heterogeneity. Parker et al. (11) even observed fractal heterogeneities in a three-dimensional branching model with equal branch flows. However, their model only relies on rules for branching without a

Address for reprint requests and other correspondence: M. Marxen, Dept. of Medical Biophysics, Sunnybrook and Women's College Health Sciences Centre, Univ. of Toronto, S605-2075 Bayview Ave., Toronto, ON, Canada M4N 3M5 (E-mail: michael.marxen@utoronto.ca).

The costs of publication of this article were defrayed in part by the payment of page charges. The article must therefore be hereby marked "*advertisement*" in accordance with 18 U.S.C. Section 1734 solely to indicate this fact.

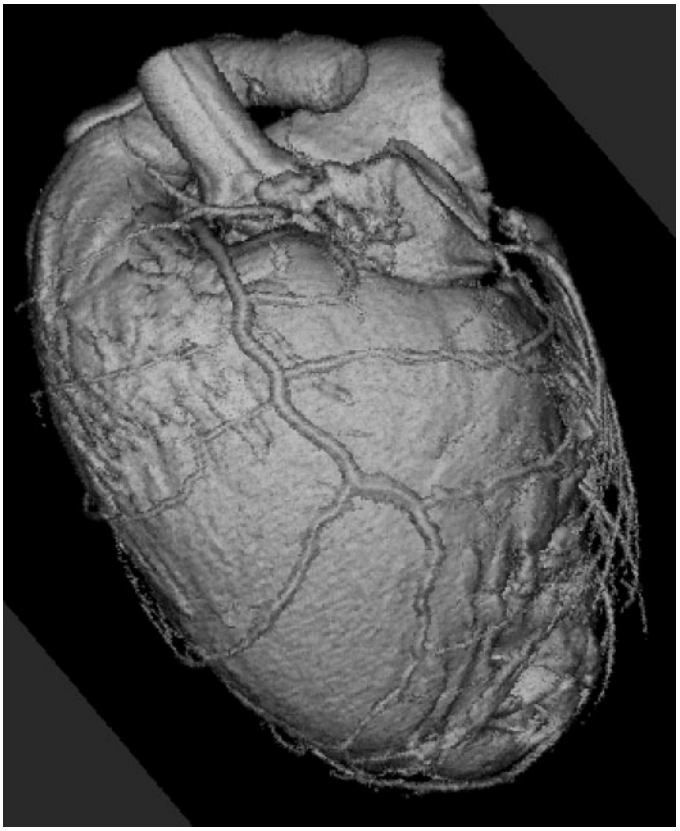

Fig. 1. Rendering of a microCT image of a mouse heart. Vessels and heart chambers are filled with X-ray contrast agent. The branching structure of a coronary vessel is clearly visible. The figure illustrates that vessel branching is highly asymmetric and that large variations in the distances from the feeding artery to the terminal vessels exist.

mechanism to distribute vessels homogeneously in space.

Alternatively, van Beek et al. (17) proposed a simple fractal flow bifurcation model, which assumes that bifurcating vessels perfuse identical volumes of tissue but carry different amounts of flow. The van Beek model does not include information on the three-dimensional distribution of vessels within the organ. Although the reported experimental data can be fitted with this model, the assumption that both branches of a bifurcation feed the same tissue volume is not physiologically realistic (20).

The proposed model links global properties of vascular structure and multiscale perfusion measurements, which may eventually lead to new interpretations of clinical perfusion data. For example, vascular changes over time or in response to stress or vasodilation in diseases like ischemic heart disease, arteriosclerosis, hypertension, diabetes, and others could be analyzed in terms of the model parameters. Other applications could be the characterization of vascular beds with differing physiology and new ways of categorizing vascular development in mutant animals.

METHODS

Relative dispersion and fractal power laws. The degree of perfusion heterogeneity is commonly quantified by measuring relative dispersion (RD; also called the coefficient of variation), defined as the standard deviation of perfusion measurements in local volumes of defined size divided by the average of these measurements. It has been found that the decrease of RD with increased mass m of the volume elements can be described by a power law function (2, 17)

$$\mathrm{RD}(m) = m^b \cdot \mathrm{RD}(1) \qquad (1)$$

Equation 1 is indicative of self-similarity, a basic property of fractals. To understand the concept of self-similarity, let us consider some quantity f: f is considered self-similar if its value measured at an arbitrary scale r differs from the value measured at the scale $n \cdot r$ only by a constant scaling factor k, which is independent of r

$$f(n \cdot r) = k \cdot f(r) \qquad (2)$$

For example, the number of vessels visible in the field of view of a microscope may increase by a factor of $k = 3$ as one zooms in and magnification is increased by a factor of $2(n = ½)$. The power law for relative dispersion of perfusion (*Eq. 1*) is consistent with the above definition of self-similarity, with the measured quantity f being the relative dispersion of perfusion RD, m equivalent to the resolution r, and b the scale-independent slope of RD vs. m on a log-log plot resulting in $k = n^b$. If perfusion is measured at a single scale m (mass of individual volume elements), relative dispersion values at scale $n \cdot m$ can then be obtained by aggregating n neighboring volume elements.

It can be shown (17) that the exponent b is related to other measures such as the fractal dimension D of the system or alternatively to C, the correlation coefficient between neighboring perfusion measurements P_1 and P_2

$$b = 1 - D = -½ + ½ \log_2 (C + 1)$$

where

$$C = \frac{\langle (P_1 - \langle P_1 \rangle) \cdot (P_2 - \langle P_2 \rangle) \rangle}{\sqrt{\langle (P_1 - \langle P_1 \rangle)^2 \rangle \langle (P_2 - \langle P_2 \rangle)^2 \rangle}} \qquad (3)$$

For a spatially random and uncorrelated distribution of perfusion ($C = 0$), a plot of log(RD) vs. log(m) results in a straight line of slope $-½$. Experimental values for b, however, indicate a positive correlation between neighboring perfusion values ($-½ < b < 0$).

Defining scale through volume ordering. The observation of fractal perfusion heterogeneities brings up interesting questions: Is the geometry of the underlying vascular structure that distributes blood flow also fractal? And does fractal perfusion heterogeneity arise from fractal vascular geometry? It is important to realize that fractal perfusion heterogeneities are by no means an obvious consequence of fractal vascular geometry and vice versa. To proceed, we need to define what we mean by fractal geometry. Here, fractal vascular geometry refers to the assumption that vessel properties like length, diameter and resistance follow power laws similar to *Eq. 1*. Vessel length is defined here as the distance between two successive branching points, often referred to as the length of a vessel segment (9).

For fractal analysis, it is important that scale of the quantity under examination is well defined. For perfusion measurements, scale has been defined through the mass of the tissue samples. For properties of vessels, we suggest a similar definition of vessel scale as the volume of tissue that is supplied by a particular artery or drained by a vein. This interpretation of scale leads to a new ordering scheme for the morphological classification of vessels. Given a branching

tree structure, different kinds of ordering schemes have been developed that attempt to group functionally equivalent tree segments by assigning them the same integer order number. In the commonly used Strahler scheme (15), terminal branches are assigned order 1 and subsequent branches are assigned the maximum order number of the daughter branches or the next higher integer number if the orders of both daughter branches are the same (see Fig. 2). One of the reasons for the success of the Strahler scheme is that the relative change of vessel diameter and length from one order to the next has been found experimentally to be a constant for a number of vascular systems (12)

$$\frac{f'(u+1)}{f'(u)} = k \tag{4}$$

where $f'(u)$ is the average length or diameter of a vessel at order u and k is a constant. Relations of this type are also known as Horton's laws. *Equation 4* is equivalent to *Eq. 2* if we postulate that $u = \log_n(r)$, meaning that Strahler order equals the logarithm of the scale of a vessel. Then the quantity f' can be expressed as a function of scale $r = n^u$

$$f'(u) = f(n^u) = f(r) \tag{5}$$

and

$$f(r) = f(1) \cdot r^{\log(k)/\log(u)} \tag{6}$$

Thus vessel length and diameter are fractal quantities if Strahler order represents scale. It would not be surprising that Strahler order is related to geometric scale because Strahler order was initially designed to classify segments of riverbeds in terms of the area of land that they are draining (15). This concept is equivalent to classifying veins in terms of the tissue volume V that they drain or arteries in terms of the volumes that they perfuse. Defining scale through tissue volume

$$r = \mathrm{V} \Rightarrow u = \log_n(\mathrm{V}) \tag{7}$$

is also physiologically reasonable because, if only geometric information is available, the most obvious parameter that characterizes the importance of an artery is the tissue volume that it supplies.

Thus we propose a new ordering scheme, which defines the volume order number U_{vol} of a vessel as a function of the supplied tissue volume V as

$$U_{\mathrm{vol}} \equiv \log_2 \mathrm{V} + 1 \tag{8}$$

An offset of 1 has been chosen to match Strahler ordering for symmetric trees assuming that the volumes fed by terminal vessel segments are normalized to 1.

An advantage of Strahler ordering is that it solely relies on topology, whereas volume ordering requires knowledge about the supplied tissue volume. In morphological studies, for example, in the analysis of vascular corrosion casts, the fed volume could be determined by simply assigning a fed volume of unity to all terminal branches, assuming a spatially invariant density of terminal vessels. This scheme would be somewhat inaccurate but, like Strahler ordering, purely topological. More complicated procedures to determine supplied volumes have only become possible through modern imaging and computer technologies. The boundary between volumes fed by neighboring terminal vessels can now be determined by a computer algorithm based on digital three-dimensional image data. The precise location of the volume boundary becomes insignificant as volumes are added up for higher-order branches.

Obviously, noninteger order numbers occur for V not being a power of 2, which will be the case for asymmetric trees. However, if so desired, a grouping of vessels into integer volume order categories can easily be done.

In this section, the discussion only refers to the conventional definition of Strahler ordering. Other authors have introduced certain refinements of the Strahler scheme such as, for example, diameter-defined Strahler ordering (9). For the purpose of this article, it is only important that a logarithmic relationship to the supplied tissue volume (*Eq. 7*) exists, which is a reasonable assumption even for diameter-defined Strahler order.

Proposed model of vascular architecture and flow. To simplify the complicated nature of vascular systems, the follow-

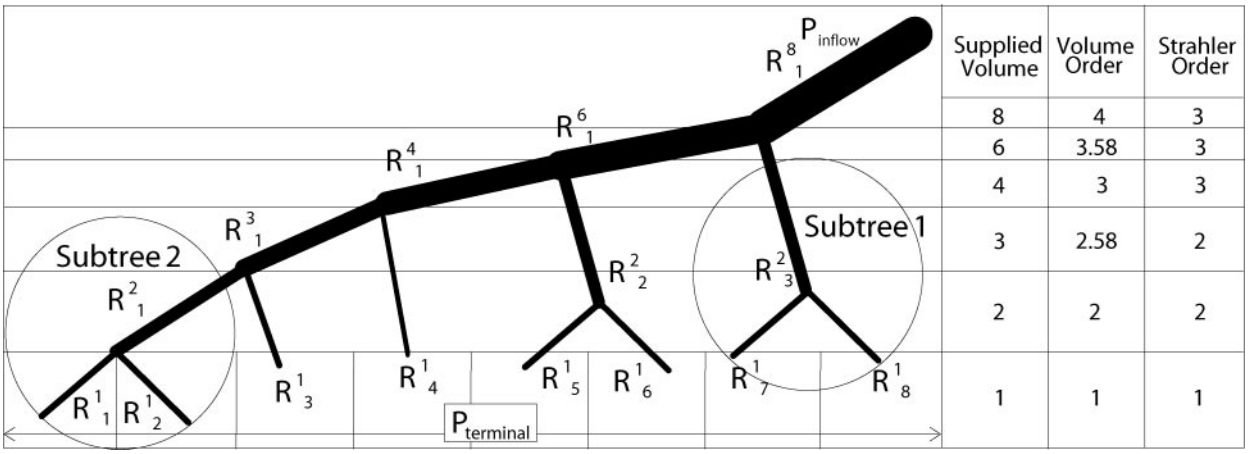

Fig. 2. Schematic illustrating the major features of the vascular model. R_i^{V} marks the resistance of a vessel segment, where V is the tissue volume being supplied by the vessel and i is a counting index for equivalent vessels. In this discrete version of the model, all tissue volumes being fed by terminal vessels are of size 1. *Subtrees 1* and *2* are feeding the same volume of tissue and represent the same resistance to blood flow. However, *subtree 1* will exhibit higher perfusion than *subtree 2* because of its higher entrance pressure. To the right of the model tree, supplied tissue volume, volume order [= $\log_2$ (supplied volume) + 1] and Strahler order of the vessels ending in the marked bands are tabulated. P_{inflow}, entrance pressure; P_{terminal}, exit pressure.

ing approximations will be used, which have previously been used by others. The vasculature is considered to be a bifurcating tree with a single feeding vessel at entrance pressure P_{inflow} and a constant exit pressure $P_{terminal}$ at the capillary level (5, 14, 16). The flow F through a vessel is computed by dividing the pressure difference ΔP between inflow and outflow by the resistance R of the vessel following Poiseuille's law. Branching asymmetry δ within the model is defined as $\delta = V_1/(V_1 + V_2)$, where V_1 and V_2 are the tissue volumes being fed by the child branches of a vessel bifurcation with $V_1 < V_2$, i.e., $0 < \delta \leq 0.5$. The volume supplied by an arbitrary branch of the vessel tree can be computed as the sum of all volumes fed by its individual terminal branches.

Two novel assumptions about vascular structure are introduced, which are the bases of the proposed model. *Assumption 1* is that vascular geometry is statistically homogeneous throughout the organ, meaning that subtrees supplying the same volume have similar geometry and resistance independent of their location. This assumption is actually implicit in many morphological studies of vessel length and diameter, which are based on ordering schemes that are not dependent on spatial location. The assumption is supported by observations that, for example, capillary and arteriolar densities in the endocardium are not significantly different from those in the epicardium (18). Figure 2 is a simplistic schematic of the model with equal terminal fed volumes. It illustrates that *assumption 1* combined with the presence of branching asymmetry is already sufficient to explain perfusion heterogeneity and the positive correlation of perfusion. The *subtrees 1* and *2* indicated are both supplying the same volume and have the same resistance, but flow in *subtree 2* will be less than flow in *subtree 1* because blood has to pass through more vessel segments before it reaches *subtree 2* than blood feeding *subtree 1*. This means a reduction of the inflow pressure for *subtree 2*. Because capillary pressures, resistances, and supplied volumes are the same, flow as well as perfusion will be reduced. This has the interesting consequence that regions of tissue being fed by the larger daughter vessel and receiving more flow at a bifurcation are actually less perfused because more flow is distributed over a disproportionally larger volume [opposite to the prediction of the model proposed by van Beek et al. (17)].

The positive correlation of perfusion in neighboring volume elements is a result of the fact that two neighboring regions of tissue are likely to be a similar vessel path length away from the feeding artery and would therefore have similar entrance pressure and perfusion. It is important to realize, however, that the model does not simply create a constant perfusion gradient in space, which would not result in fractal perfusion heterogeneity. The heterogeneity exists on all scales and increases as the sample element volumes decrease.

Another assumption needs to be introduced to verify the scale independence of the correlation between neighboring perfusion values via a direct calculation of relative flow and dispersion. *Assumption 2* is that vascular geometry is fractal, meaning that branching asymmetry δ is independent of scale and vessel resistance R is a power law function of the supplied tissue volume: $R \propto V^{-q}$, where q is a fractal scaling parameter. In this article, the term "vessel" always refers to a vessel segment between two successive branching points. Vessel resistance R only refers to the resistance of a segment and not to the resistance of a whole subtree. Note that a fractal model in which subtree conductance, the inverse of resistance, and thus flow are proportional to the supplied tissue volume would actually lead by definition to homogeneous perfusion that is not observed experimentally.

The power law behavior of vessel resistance is based on the hypothesis that both vessel diameter d and length l individually follow power law behavior as a function of volume scale with respective scaling parameters s and t

$$d(V) \propto V^s, \quad l(V) \propto V^t \Rightarrow l \propto d^{t/s} \tag{9}$$

If we accept the relation between scale and Strahler order postulated above (*Eq. 7*), these relations are equivalent to Horton's laws (*Eqs. 4* and *6*) and are justified for a number of organs (12), including the heart (9). Given that fed volumes are additive, note that a value of $s = 1/3$ is equivalent to Murray's law (10), which states that the sum of the cubes of the vessel diameters is conserved at bifurcations.

Assuming laminar, nonpulsatile flow and constant blood viscosity, the resistance R of a vessel segment is according to Poiseuille's law

$$R \propto \frac{l}{d^4} \propto V^{t-4s} \propto V^{-q} \tag{10}$$

where $q = 4s - t$. West et al. (19) have suggested $t = 1/3$ for a space-filling, fractal vasculature and $s = 1/3$ for nonpulsatile flow resulting in $q = 1$.

Experimental data on vascular geometry and hemodynamics are often expressed in the literature in terms of vessel diameter rather than fed tissue volume. Experimental data gathered by Kassab et al. (9) and vanBavel and Spaan (16) suggest a value of ¾ for the exponent t/s in the power law of vessel length l as a function of vessel diameter d (*Eq. 9*). This value of t/s seems to be experimentally better established than a value of s = 1/3 (19). Using $t/s = ¾$ and $q = 4s - t$ (*Eq. 10*), we can rewrite *Eq. 9* as

$$d \propto V^{4q/13} \tag{11}$$

This expression can now be used to compare the asymmetry parameter δ with the parameter α, which has been defined by Zamir (20) as the ratio of the smaller diameter d_2 over the larger diameter d_1 of the daughter vessels of a bifurcation

$$\alpha = \frac{d_2}{d_1} = \left[\frac{\delta \cdot V}{(1-\delta) \cdot V}\right]^{4q/13} \tag{12}$$

Figure 3 illustrates the meaning of the parameters δ and q. Although the meaning of the asymmetry parameter is fairly obvious, it is important to realize the scaling properties governed by q. An increase in q can be thought of as more rapid shrinking of the vessel diameter. Figure 4 illustrates the effect of q for a symmetric branching tree with 21 generations. Normalized pressure is plotted as a function of volume order. Note that normalized pressure at a certain order is equivalent to the cumulative relative resistance of all lower levels. In the case of symmetric branching, one can think of each level contributing in series to the total resistance. A q of 1.0 means that vessel conductance is proportional to the supplied volume, which is, in total, the same for each level. Thus the total conductance of vessels of a certain order is the same for all order numbers and the pressure drop is constant at each level. As q increases, the relative resistance in vessels of low orders increases as well as the relative pressure drop. This basic rule also holds for the average pressure in asymmetric branching trees. However, the pressure distribution for asymmetric trees is more complicated than in the symmetric case because different pressures are possible for the same supplied volumes depending on the distance of the vessel from the root of the tree structure.

Model implementation. A flow chart of the computational steps that are involved in the implementation of the proposed

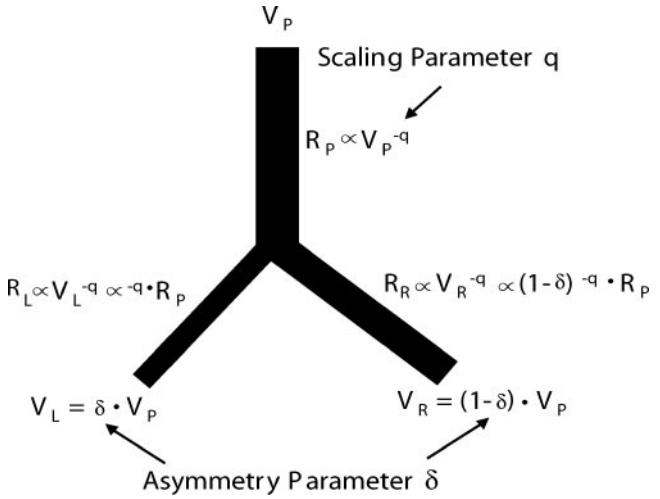

Fig. 3. Illustration of the effects of the asymmetry parameter δ and the scaling parameter q. V_P and $V_{L,R}$, and R_P and $R_{L,R}$, mark the volume being fed by, and the resistance of, the parent and child vessels, respectively; δ determines the asymmetry of the tissue volumes that are being fed by the branches of a bifurcation (δ = 0.5 represents total symmetry). The parameter q governs the increase of resistance, which can be interpreted as a decrease in diameter.

model is given in Fig. 5. A typical simulation requires four steps: *1*) construction of the vascular tree according to the chosen input parameter set, *2*) calculation of flow and pressure distribution within the network, *3*) uniform division of outflow volumes (voxelation), and *4*) calculation of relative dispersion at different levels of aggregation.

The input parameters are in boldface in the flow chart for easy identification. The asymmetry δ and the scaling parameter q are described in detail above. Additional parameters are the total supplied tissue volume V_0 and the minimum volume V_{min}, below which branching does not occur any further. V_{min} was set to $2/(1 + \delta)$, which resulted in a mean volume fed by terminal vessels of ~1. This is just a choice of convenience. The real values in cubic millimeters do not matter for the simulations. However, the ratio V_0/V_{min} should be chosen to be realistic for the system being simulated (see below).

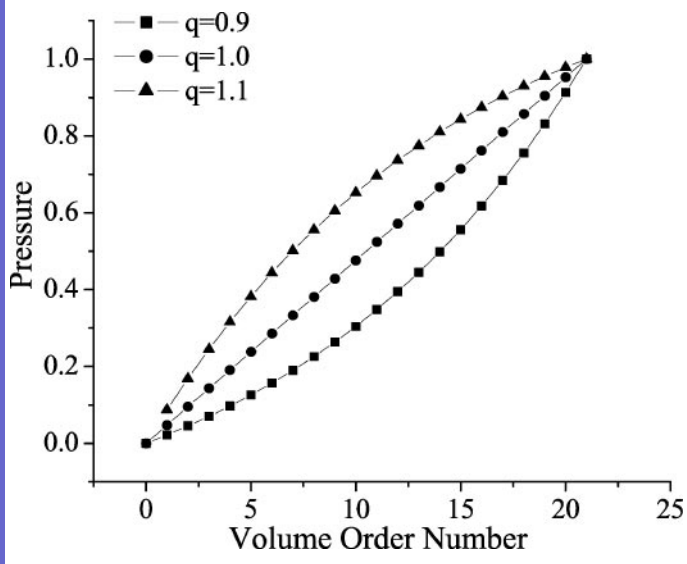

Fig. 4. Illustration of the effect of the resistance scaling parameter q. Normalized pressure is plotted as a function of volume order number for a symmetrically branching tree with 21 generations. As q increases, more pressure is lost in vessels of low order.

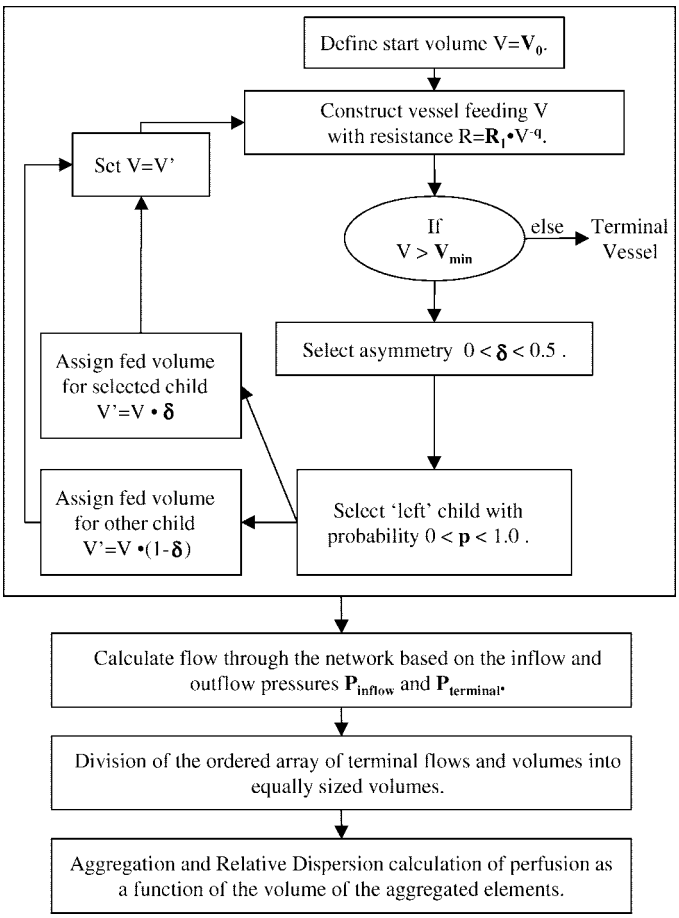

Fig. 5. Flow chart of the algorithm used to implement the presented model. Model parameters are in boldface.

Further parameters are the resistance of a vessel R_1 feeding one unit of volume and the inflow and terminal pressures P_{inflow} and $P_{terminal}$. It is important to recognize that these three parameters influence only the absolute flow through the vascular network. The relative dispersion is independent of these parameters. This is an advantage of relative dispersion analysis because knowledge of absolute flow and pressure is not required.

Finally, the parameter p is the probability with which the "left" vessel is being chosen as the smaller one. A value of p = 0.5 is equivalent to assigning fed volumes in a totally random fashion to the "left" or "right" child vessel. "Left" and "right" are framed by quotation marks because these terms are not applicable in three dimensions. p can generally be viewed as a measure of directional bias of the asymmetry. It will be shown that the results are independent of p.

For the calculation of flow, the total resistance $R_{subtree}$ of the structure in Fig. 3 can be expressed as

$$R_{subtree} = \frac{R_L \cdot R_R}{R_L + R_R} + R_P \qquad (13)$$

where R_P and $R_{L,R}$ are the resistances of the parent and child vessels, respectively. Given the resistance of all vessel segments from *step 1* (see Fig. 5), this formula is used in a recursive fashion to calculate the resistances of all subtrees

within the network (*step 2*). Flows and pressures for each subtree and segment can be calculated given the inflow pressure P_{inflow} and the terminal pressure $P_{terminal}$.

The resulting flows F_i through each terminal branch together with the volumes V_i that are being fed are arranged in a vector $[\ldots, (F_{i-1}, V_{i-1}), (F_i, V_i), (F_{i+1}, V_{i+1}), \ldots]$ according to their proximity in the tree (see Fig. 2), meaning that child branches in the tree will be neighbors in the vector. In an experiment, perfusion measurements are usually done in sample volumes (voxels) of equal size. The volumes V_i, however, vary in size. Thus in *step 3*, a volume vector is created with volumes V'_i of equal size, which intersect one or more (most commonly 2) volumes of the original vector. Therefore, the associated flows F'_i are calculated as the properly weighted average flow in all intersected volumes.

Finally, the relative dispersion of perfusion is calculated as the standard deviation divided by the mean of F'_i. This is done on different scales m by aggregating neighboring vector elements so that $F'^{m}_i = F'^{m/2}_{2i} + F'^{m/2}_{2i-1}$. This is very similar to the procedure used by van Beek et al. (17).

RESULTS

Initially, the independence of the relative dispersion of perfusion from the parameters R_1, P_{inflow}, and $P_{terminal}$ was verified (data not presented). The other parameters V_0, V_{min}, p, δ, and q have been set to 1,048,576, $2/(1+\delta)$ (see *Model implementation*), 0.5, 0.1, and 1.0, respectively, unless noted otherwise. These values have been chosen to approximately match experimental data in sheep hearts demonstrating the capacity of the proposed model to generate physiologically reasonable data. Bassingthwaighte et al. (3) have published relative dispersion data on myocardial perfusion in 11 sheep. The average relative dispersion of perfusion as measured with the soluble flow marker 2-iododesmethylimipramine was 33%, ranging from 16% to 47% in individual animals for 254 tissue pieces averaging 217 mg. Aggregation of adjacent pieces resulted in fractal dimensions ranging from 1.07 to 1.30 with a value of 1.16 for the composite data. The number of vessels in the model tree should be sufficient to represent all vessels from the feeding artery to the small arterioles. Kassab et al. (9) have presented data on the number of vessels in pig hearts. Assuming a pig heart weight of ~105 g, they found ~27,900 vessels above 9 μm in diameter per gram of tissue. Assuming that this number includes the terminal arterioles and that vessel density ρ_v scales with animal weight W to the power of −1/4 (19), the relevant number of vessels N in the sheep heart can be estimated to be

$$\rho_v(\text{sheep}) = \rho_v(\text{pig})\left[\frac{W(\text{sheep})}{W(\text{pig})}\right]^{-1/4} = 27{,}900\,\frac{1}{\text{g}}\cdot\left[\frac{18.4\text{ kg}}{30\text{ kg}}\right]^{-1/4} = 31{,}527\,\frac{1}{\text{g}} \Rightarrow$$

$$N = \rho_v(\text{sheep})\cdot W(\text{sheep heart}) = 31{,}527\,\frac{1}{\text{g}}\cdot 62.5\text{ g} \approx 1{,}970{,}400$$

In the simulations, we have chosen V_0 to be 2^{20} = 1,048,576, which results in generating ~2^{21} = 2,097,152 vessels. The average weight of tissue fed by a terminal vessel is ~0.06 mg, equivalent to a volume of ~(400 μm)^3. The sample element masses in the experimental data of 217 mg up to 9.6 g are thus approximately equivalent to aggregating 3,600 and 160,000 elements, respectively. Therefore, only relative dispersion values in the simulations from 2,048 to 131,072 aggregated sample elements have been used in an attempt to match the experimental data. Relative dispersion values have not been calculated for sample element volumes >131,072 or <8 sample elements because determination of a standard deviation from only 4 values is unreliable.

Figure 6 shows the logarithm of relative dispersion of perfusion as a function of sample element volume and illustrates the influence of the two major parameters of the model, the asymmetry parameter δ and the scaling parameter q. Values of $q = 1.0$ and $\delta = 0.1$ result in a fractal dimension $D = 1.15$ and a relative dispersion RD of 0.35 at a relative sample volume of 2,048. These values are very close to the average values quoted above for the sheep heart. Both these values for q and δ are physiologically reasonable: $q = 1.0$ is the expected value for nonpulsatile, laminar flow as predicted by West et al. (19), and the asymmetry parameter $\delta = 0.1$, which is equivalent to $\alpha = 0.51$ ($q = 1.0$ in *Eq. 12*), falls within the expected range based on data presented by Zamir (20) for distributing vessels in the human heart, which feed large volumes of tissue.

It can be noted in Fig. 6*A* that a variation of δ in a range from 0.05 to 0.3 only affects the intercept of the RD curve but not its slope. Of course, this behavior will break down if δ is chosen to be very close to 0.5. This is only of theoretical concern, though, because any variance in δ will result in a reduction of the mean value of δ below 0.5. In contrast, Fig. 6*B* indicates that a variation of q induces a change in the slope as well as the y-axis intercept. The observation of Bauer et al. (4) that vasodilation changes fractal dimension or the slope of the RD curve could thus be interpreted as a change in the parameter q.

Another interesting finding is that the data in Fig. 6*A*, if plotted as a function of asymmetry δ for different sample element volumes (plot not shown), can be well approximated by an exponential function in the range $0.1 < \delta < 0.35$ for sample element volumes of 32,768 and smaller. Thus the estimation of the asymmetry based on RD data is very easy in this parameter region. The distinct difference in the action of the two parameters δ and q allows for a very stable fit of experimental data. The large variations in both the absolute RD values and the fractal dimension of the experimental

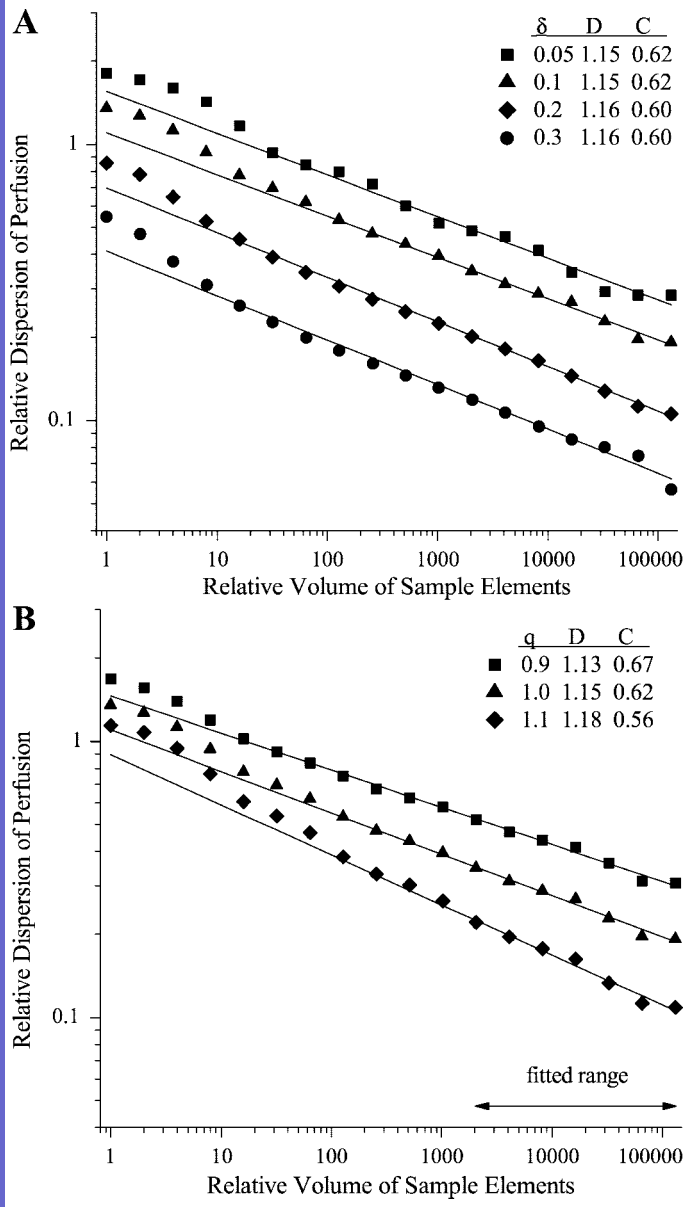

Fig. 6. Log-log plots of the relative dispersion (standard deviation/mean) of perfusion as a function of relative sample element volume (RD plots) for different asymmetry parameters δ (*A*) at $q = 1.0$ and different scaling parameters q (*B*) at $\delta = 0.1$. RD was computed from 1,048,576 volumes at a relative sample element volume of 1 and from 8 volumes at a relative sample element volume of 131,072. Relative sample element volumes of 2,056 to 131,072 have been fitted with power law functions resulting in the given fractal dimensions D and the correlation coefficients between neighboring volumes C. The fractal dimension D is equivalent to 1 minus the slope of the curves.

data (3) indicate that it might be possible to distinguish the underlying vascular morphologies in terms of their asymmetry and resistance scaling.

Although the presence of branching asymmetry is hardly disputable, the scale independence of the asymmetry is only an approximation and seems to change between distributing vessels, which are feeding large volumes of tissue, and delivering vessels, which are supplying small regions (20). In Fig. 7, the effect of a change of δ from 0.1 to 0.4 for vessels feeding a volume less than the variable parameter $V_{\delta\text{-switch}}$ is investigated. The δ values of 0.1 and 0.4 have been chosen to represent distributing ($\alpha = 0.51$) and delivering ($\alpha = 0.88$) vessels, respectively (20). A decrease of the RD values for fed volumes below $V_{\delta\text{-switch}}$ can be observed. The slope of the curve above $V_{\delta\text{-switch}}$ remains unchanged. However, measurements in the rat heart (4) and rat lungs (6) show that perfusion heterogeneities remain fractal down to very small scales. This may indicate that fluctuations in branching asymmetry may be modeled by random fluctuations about a mean value rather than by a distinction between delivering and distributing vessels.

The parameter p of the proposed model determines the probability that the smaller fed volume will be assigned to one of the child vessels. An equally likely assignment to either child ($p = 0.5$) would represent a very different three-dimensional arrangement of vessels than assigning the smaller fed volume always to the right child ($p = 0.0$). Relative dispersion curves for different values of p are plotted in Fig. 8. It can be seen that the effect of p on the relative dispersion curves is insignificant. This finding indicates that knowledge of the three-dimensional distribution of vessels, which is ignored in this model, might not be necessary to account accurately for perfusion heterogeneity. The validity of this interpretation remains to be shown by comparison with realistic three-dimensional models.

An important consideration in evaluating the utility of a model is the effect of noise in the parameter space. Small levels of noise should not have a significant influence on model outcome. A true biological vasculature will not exhibit strict self-similarity. The values for δ and q for vessels feeding the same volume will fluctuate around a mean value. Simulations were performed to examine changes in the RD curves for noise in the resistance and branching asymmetry of a vessel.

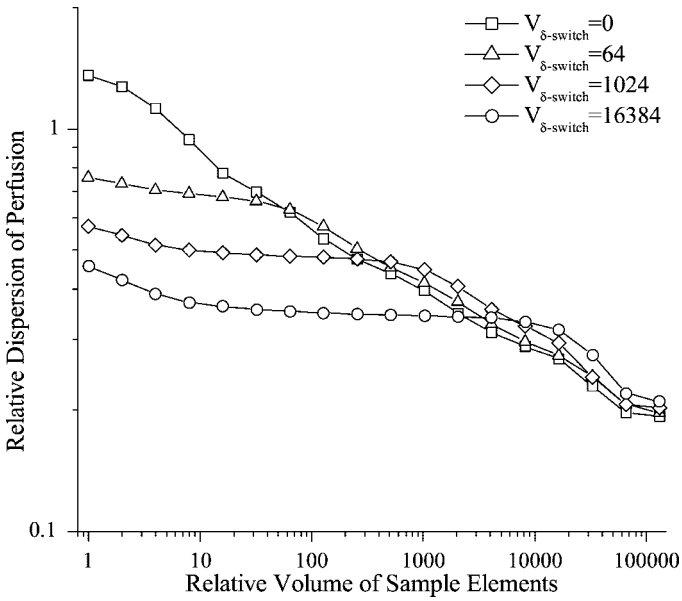

Fig. 7. RD plot with the asymmetry parameter δ set to 0.4 for $V < V_{\delta\text{-switch}}$ and 0.1 for $V > V_{\delta\text{-switch}}$.

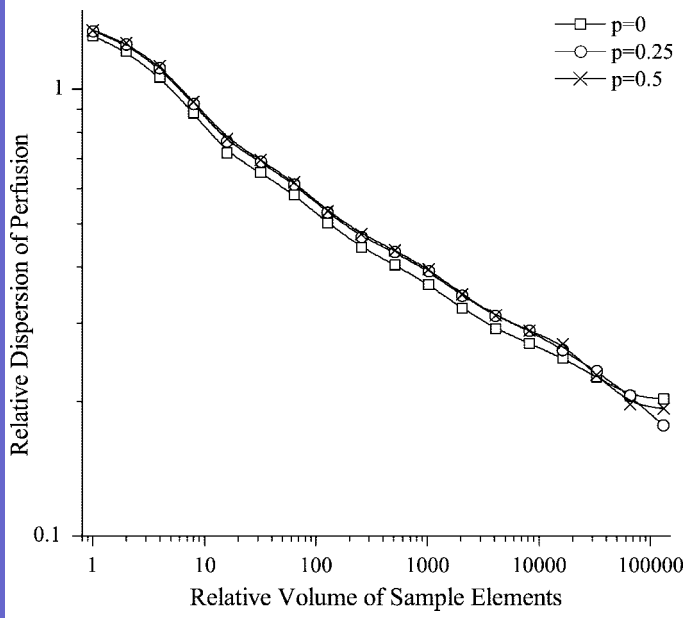

Fig. 8. RD plot for 3 parameters p, which governs the probability of assigning the larger fed volume to a specific branch of a bifurcation. Only a small change can be noted for totally random ($p = 0.5$) assignment vs. the totally deterministic ($p = 0.0$) case.

The parameter δ and the conductance of a vessel $C = 1/R$ were chosen randomly from distributions with means $\bar{\delta}$ and $\bar{C} = V/R_1$. The degree of variability in these parameters was defined by the standard deviation σ_δ of δ and the relative standard deviation $\sigma_C/\bar{C}$ of C. A normal distribution with $\sigma_C/\bar{C} = 0.3$ with $C > 0$ resulted in a relative standard deviation of the RD values of 8% for nine different seed values at a relative sample element volume (RSEV) of 131,072, which dropped below 2% for RSEV < 4,096. The average over all RSEVs of the absolute deviation of the mean value from the noiseless RD value was 4.5%. To generate a worst case scenario for the variation in δ, a highly asymmetric distribution $\rho(\delta) = 0.0253 \cdot \delta^{-2.4}$ for $0.053 < \delta < 0.288$ with $\bar{\delta} = 0.1$ and $\sigma_\delta = 0.05$ was chosen. The relative standard deviation of the RD values was 12% for nine different seed values at a RSEV of 131,072, which dropped below 2% for RSEV < 2,048. The average over all RSEVs of the absolute deviation of the mean value from the noiseless RD value was 3%. Thus a reasonable amount of noise in the simulation resulted in only small changes to the relative dispersion values.

To demonstrate an important property of volume ordering, average volume order of all vessels with the same Strahler order is plotted vs. Strahler order in Fig. 9. For symmetric branching ($\delta = 0.5$), volume and Strahler order are equivalent, resulting in a line slope of 1. Obviously, the postulated relationship $u_{\text{Strahler}} = \log_n(V) + 1 = (U_{\text{vol}} - 1)/\log_2 n + 1$ (*Eqs. 7 and 8*) is not precise for asymmetric branching because Strahler orders are integer valued. Figure 9 shows that, in an average sense, the logarithmic relationship between Strahler order and supplied tissue volume even holds for asymmetric trees as long as the asymmetry is constant at all branch points. However, the line slope increases as asymmetry is increased from 0.5 to 0.1, indicating that $n = 2^{(\text{line slope})}$ also increases. Consequently, it is not possible to infer the volume being fed by a vessel or its absolute scale from its Strahler order without specifying the asymmetry of the vascular system. Thus an analysis based on Strahler order will indicate fractal behavior of systems with constant branching asymmetry, but it is not adequate for fractal analysis of tree structures with changing asymmetry or comparison of fractal dimensions of branching systems with different asymmetry. In contrast, fractal dimensions based on volume ordering are independent of branching asymmetry.

DISCUSSION

If perfusion heterogeneity is fractal and exhibits a power law behavior, its scale dependence can be described by only two parameters. However, slope and intercept on a double-logarithmic plot do not reveal the design properties of the underlying vascular structure. The presented model allows a reasonable interpretation of multiscale perfusion heterogeneity data in terms of two morphological parameters δ and q describing branching asymmetry and scaling of vessel resistance. It is obvious that two parameters are not sufficient to capture the whole complexity of vascular morphology, but these two parameters contain important physiological concepts that are shown to be of major importance in understanding the remarkable fractal properties of perfusion heterogeneity.

Extensions of the presented model are certainly possible. Examples would be the effect of gravitation on the pressure distribution or a more complicated model of blood flow including pulsatility of flow or the reduction of blood viscosity in small vessels (7, 13). Gravitational influences are expected to be relatively small (7).

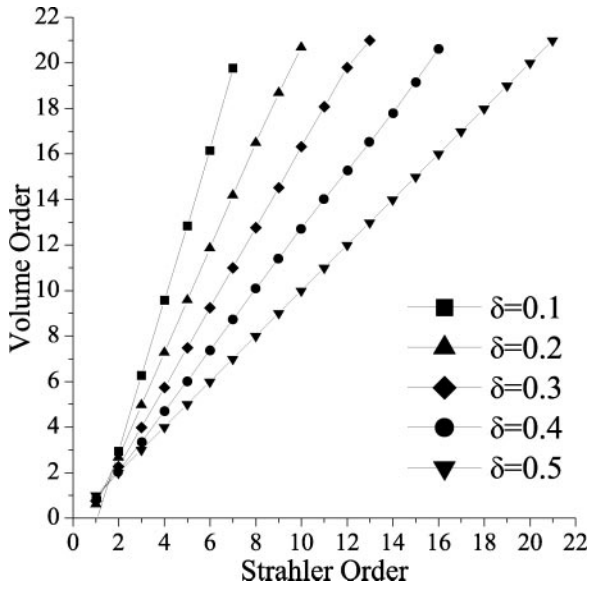

Fig. 9. Plot of average volume order vs. Strahler order for different asymmetry parameters δ.

For pulsatile flow, the anticipated value for s would be ½, which would result in $q = 5/3$ according to West et al. (19). Given that q has been determined to be ~1.0, pulsatility of flow seems to be of minor importance in sheep hearts.

We have argued above that fractal relationships for the length and diameter as a function of scale exist. However, the data gathered by Kassab et al. (9) and vanBavel and Spaan (16) show a large degree of fluctuation of length and diameter measurements. More realistic statistical distributions could be applied in the construction of the vascular tree. It should be noted that a possible correlation of the observed deviations from the expected mean with the distance from the feeding vessel could potentially reduce flow heterogeneities. These correlations have not yet been studied in detail.

Three-dimensional structure could be added to the model, but it is important to realize that every additional parameter in the model will make it more difficult to think about fractal perfusion heterogeneities conceptually. In addition, Glenny and Robertson (7) found that perfusion heterogeneity from a three-dimensional simulation agreed with results based on the aggregation method used by van Beek et al. (17), which is equivalent to the one presented here.

The model currently allows a qualitative understanding of how branching asymmetry and the distribution of vessel resistance influence perfusion heterogeneity. Better data on three-dimensional vascular geometry are still needed to examine the exact meaning of the average parameters δ and q as well as to validate the assumption of fractal vascular architecture. Comparison with calculations of relative dispersion of perfusion for a realistic, fully three-dimensional vascular model would also be helpful in this context. To obtain the required data, we are currently studying vascular structure with microcomputed tomography (see Fig. 1). Ideally, one would like to perform a perfusion study with calculation of relative dispersion, extract structural information from a three-dimensional image of the vasculature, and use this to validate the model parameters that have been fitted to the experimental perfusion data. Experiments of this kind will be useful to compare structure and properties of the model tree with those of real vascular trees.

In conclusion, a vascular model based on asymmetric branching and fractal vascular structure has been introduced, which defines branching asymmetry based on the tissue volume that is fed by each vessel. Following the concept of fed tissue volume, a logarithmic volume ordering scheme for vessels is proposed. Fractal dimensions of vascular systems can be compared within this scheme independent of the branching characteristics of the vasculature.

It is shown that the model is able to explain the observed heterogeneity of perfusion and the positive and scale-independent correlation between neighboring perfusion values in organs such as the heart. The two major parameters of the model specify the branching asymmetry of the vasculature and the scaling properties or fractal dimension of vessel resistance. Simulations indicate that branching asymmetry only increases the magnitude of the relative dispersion of perfusion but does not influence its spatial correlation. However, the resistance scaling parameter is related to both the magnitude of relative dispersion and the correlation of perfusion. It is shown that as relative resistance shifts from larger toward smaller vessels, heterogeneity and correlation decrease. The model parameters have been matched to perfusion data in the sheep heart. The results fall within the physiologically expected range. More detailed three-dimensional data on vascular morphology are needed to verify the model assumptions. The model assists in the interpretation of noninvasive perfusion imaging techniques like PET or MRI, allowing the characterization of vascular morphology without acquiring direct information about vascular geometry. This information is very valuable for diagnosis, prognosis, and monitoring therapy response in diseases such as cardiovascular disease, diabetes, arteriosclerosis, hypertension, and cancer.

We thank Janet Koprivnikar, who provided the microCT specimen in Fig. 1.

This research is supported by the Canadian Institutes of Health Research, the National Cancer Institute of Canada, and a research traineeship (for M. Marxen) from the Heart and Stroke Foundation of Canada.

REFERENCES

1. **Bassingthwaighte JB.** Blood flow and diffusion through mammalian organs. *Science* 167: 1347–1353, 1970.
2. **Bassingthwaighte JB, King RB, and Roger SA.** Fractal nature of regional myocardial blood flow heterogeneity. *Circ Res* 65: 578–590, 1989.
3. **Bassingthwaighte JB, Malone MA, Moffett TC, King RB, Chan IS, Link JM, and Krohn KA.** Molecular and particulate depositions for regional myocardial flows in sheep. *Circ Res* 66: 1328–1344, 1990.
4. **Bauer WR, Hiller KH, Galuppo P, Neubauer S, Köpke J, Haase A, Waller C, and Ertl G.** Fast high-resolution magnetic resonance imaging demonstrates fractality of myocardial perfusion in microscopic dimensions. *Circ Res* 88: 340–346, 2001.
5. **Beard DA and Bassingthwaighte JB.** Fractal nature of myocardial blood flow emerges from whole-organ model of arterial network. *J Vasc Res* 37: 282–296, 2000.
6. **Glenny RW, Bernard SL, and Robertson HT.** Pulmonary blood flow remains fractal down to the level of gas exchange. *J Appl Physiol* 89: 742–748, 2000.
7. **Glenny RW and Robertson HT.** A computer simulation of pulmonary perfusion in three dimensions. *J Appl Physiol* 79: 357–369, 1995.
8. **Kalliokoski KK, Kuusela TA, Nuutila P, Tolvanen T, Oikonen V, Teräs M, Takala TES, and Knuuti J.** Perfusion heterogeneity in human skeletal muscle: fractal analysis of PET data. *Eur J Nucl Med* 28: 450–456, 2001.
9. **Kassab GS, Rider CA, Tang NJ, and Fung YCB.** Morphometry of pig coronary arterial trees. *Am J Physiol Heart Circ Physiol* 265: H350–H365, 1993.
10. **Murray CD.** The physiological principle of minimum work. I. The vascular system and the cost of blood volume. *Proc Natl Acad Sci USA* 12: 207–214, 1926.
11. **Parker JC, Cave BC, Ardell JL, Hamm CR, and Williams SG.** Vascular tree structure affects lung blood flow heterogeneity simulated in three dimensions. *J Appl Physiol* 83: 1370–1382, 1997.

12. **Popel AS.** Network models of peripheral circulation. In: *Handbook of Bioengineering*, edited by Skalak R and Chien S. New York: McGraw-Hill, 1987.
13. **Pries AR, Secomb TW, and Gaehtgens P.** Biophysical aspects of blood flow in the microvasculature. *Cardiovasc Res* 32: 654–667, 1996.
14. **Schreiner W and Buxbaum PF.** Computer-optimization of vascular trees. *IEEE Trans Biomed Eng* 40: 482–490, 1993.
15. **Strahler AN.** Quantitative analysis of watershed geomorphology. *Trans Am Geophys Union* 38: 913–920, 1957.
16. **VanBavel E and Spaan JAE.** Branching patterns in the porcine coronary arterial tree. Estimation of flow heterogeneity. *Circ Res* 71: 1200–1212, 1992.
17. **Van Beek JHGM, Roger SA, and Bassingthwaighte JB.** Regional myocardial flow heterogeneity explained with fractal networks. *Am J Physiol Heart Circ Physiol* 257: H1670–H1680, 1989.
18. **Weis HR and Conway RS.** Morphometric study of the total and perfused arteriolar and capillary network of the rabbit left ventricle. *Cardiovasc Res* 19: 343–354, 1985.
19. **West GB, Brown JH, and Enquist BJ.** A general model for the origin of allometric scaling laws in biology. *Science* 276: 122–126, 1997.
20. **Zamir M.** Distributing and delivering vessels of the human heart. *J Gen Physiol* 91: 725–735, 1988.